LiOH/Coconut Shell Activated Carbon Ratio Effect on the Electrical Conductivity of Lithium Ion Battery Anode Active Material

by Yayuk Astuti

Submission date: 02-May-2023 03:32PM (UTC+0700)
Submission ID: 2081879726
File name: C5-Artikel.pdf (565.67K)
Word count: 5063
Character count: 26116

MOLEKUL
www.jmolekul.com

Articles

https://doi.org/10.20884/1.jm.2021.16.3.805

LiOH/Coconut Shell Activated Carbon Ratio Effect on the Conductivity of Lithium Ion Battery Anode Active Material

Annisa Syifaurrahma, Arnelli, Yayuk Astuti*

Chemistry Department, Faculty of Sciences and Mathematics, Diponegoro University
Jl. Profesor Soedharto, S.H. Tembalang, Semarang, Central Java, Indonesia 50275

*Corresponding author email: yayuk.astuti@live.undip.ac.id

Received July 24, 2021; **Accepted** September 15, 2021; **Available online** November 15, 2021

ABSTRACT. A lithium ion battery anode active material comprised of LiOH (Li) and coconut shell activated carbon (AC) has been synthesized with Li/AC ratios of (w/w) 1/1, 2/1, 3/1, and 4/1 through the sol-gel method. The present study aims to ascertain the best Li/AC ratio that produces an anode active material with the best electrical conductivity value and determine the characteristics of the anode active material in terms of functional groups, surface area, crystallinity, and capacity. Based on the electrical conductivity test using LCR, the active material Li/AC 2/1 had the highest electrical conductivity with a value of 2.064×10^{-3} Sm^{-1}. The conductivity achieved was slightly smaller than that of the active material with no addition of LiOH on the activated carbon at an electrical conductivity of 5.434×10^{-3} Sm^{-1}. The FTIR spectra of the activated carbon and Li/AC 2/1 showed differences in the Li-O-C group absorption at 1075 cm^{-1} wavenumber and the wide absorption in the area of 547.5 cm^{-1} that represents Li-O vibration. Based on the results of SAA, the activated carbon had a larger surface area than Li/AC 2/1 at 17.057 m^2g^{-1} and 5.615 m^2g^{-1}, respectively. The crystallinity of both active materials was low shown by the widening of the diffraction peaks. Tests with cyclic voltammetry (CV) proved that there was a reduction-oxidation reaction for the two samples in the first cycle with a large charge and discharge capacities of the activated carbon of 150.989 mAh and 92.040 mAh, while for Li/AC 2/1 they were 91.103 mAh and 47.580 mAh.

Keywords: activated carbon, LiOH, lithium ion battery anode active material, electrical conductivity.

INTRODUCTION

Batteries are devices that are capable of converting chemical energy into electrical energy through electrochemical processes, namely oxidation and reduction reactions. Lithium ion battery is one type of secondary battery that has widely been developed because it has high energy density, good cycle life, and no memory effect (Yu et al., 2015). The components comprising the battery entails anode and cathode active materials, separators, and electrolytes.

The commonly used anode active material is graphite which has a theoretical capacity of 372 $mAhg^{-1}$ (Han, Jung, Jeong, & Oh, 2014). This capacity is relatively low and thus unable to adequately support the capacity need of electronic devices which are now increasing. The alternative is to use activated carbon as an anode active material instead of graphite. Activated carbon is being developed into anode material for lithium ion batteries because it has demonstrated higher capacity than graphite's theoretical capacity limit, good cycle stability, and a volumetric capacity of 1770 $mAhcm^{-3}$ (Kim et al., 2016). Research to improve the performance of activated carbon as an anode active material for lithium ion batteries continues to be carried out. Electrical conductivity can be increased by adding materials that are good electron conductors. Lithium hydroxide (LiOH) is one of the materials that can help promote conductivity since it has an average experimental conductivity of 129.05 Sm^{-1} (Corti, Crovetto, & Fernández-Prini, 1979). Lithium ion batteries in principle do not use lithium metal as an anode due to the possible formation of lithium dendrites.

Previous research using activated carbon from candlenut shells with LiOH as an electrode has been carried out by Susana and Astuti (Susana & Astuti, 2016). The optimum electrical conductivity found was 2.34×10^{-4} Sm^{-1} and the capacitance was 327.93 F. On that account, exploration of the potential source of activated carbon in electrode making is thus critical. This includes a coconut shell that has a conductivity of 95 Sm^{-1} (Yuningsih & Mulyadi, 2016).

By looking at the previous studies, in this study, the anode active material from LiOH and coconut shell activated carbon was synthesized by variation of both materials with the ratio (w/w). Such design was undertaken to determine the effect of the addition of OH on the electrical conductivity of the active material. The ratio that produced the highest electrical conductivity value was characterized for its functional groups, surface area, crystallinity, and capacity.

EXPERIMENTAL SECTION

Materials and Equipments

The equipment used in this study were glasswares, analytical balance, pyrolysis reactor, furnace, microwave, oven, hot plate magnetic stirrer, petri dish, filter paper, pH meter, 200 mesh sieve, FTIR, XRD, LCR, CV, and SAA. The materials used in this study were coconut shell, 50% KOH, PEG 6000, citric acid, LiOH, 95% ethanol, and distilled water.

Research Procedures

The present research involved four stages of synthesis and characterization. The first was the production of coconut shell-activated carbon, starting from the carbonization of coconut shell carbonization and pyrolyzed coconut shell carbon activation. The second stage was the synthesis of activated carbon into an anode active material for lithium batteries using the sol-gel method. The third stage was the electrical conductivity test of the active material using LCR meter (LCR meter HIOKI 3532-50). Furthermore, the active material was characterized using FTIR (PerkinElmer with wavenumber in the range of 400–4000 cm^{-1}), XRD (XRD Bruker which was carried out by firing the sample with X-rays of a CuKα source that has a wavelength of 1.54178 Å and a voltage of 30.0 kV), SAA (Quantachrome NOVA Instruments version 10,01), and CV (Neware Battery Analyzer) for the LI/AC sample that had the highest electrical conductivity.

Activated Carbon Production

Coconut shells were cut into small pieces, cleaned from fibers, and dried at room temperature. The dried coconut shell was carbonized through the pyrolysis method using a pyrolysis reactor at a temperature of 400 °C for 1 hour.

Anode Active Material Synthesis

Carbonized carbon was activated chemically using 50% KOH. The ratio of carbon to 50% KOH (w/v) used was 1:5. The carbon that had been soaked in 50% KOH was microwaved for 5 minutes at 400 Watt for its physical activation. The product obtained was ground and sieved with a 200 mesh sieve.

PEG 6000 was poured into a graduated cylinder glass and then dissolved in 95% ethanol at a temperature of 50 °C. The mixture of LiOH and activated carbon with the variation of ratio (w/w) 1/1, 2/1, 3/1, 4/1, and also activated carbon without the addition of LiOH were stirred and poured into a graduated cylinder glass containing PEG 6000 solution while stirring and followed by the addition of 4 M citric acid until the pH 4-5 was reached. The temperature of the mixture was then increased to 100 °C to form a gel for 1 hour and kept for 3 days. The gel was oven-dried at 105 °C for 2 hours. Furthermore, the products were calcined at a temperature of 300 °C to remove the water content and other organic substances.

Active Anode Material Characterization

The active material was tested for electrical conductivity using an LCR meter. The ratio of LiOH to activated carbon (Li/AC) that had the highest electrical conductivity was further characterized and made into battery cells. The characterizations used were FTIR, XRD, and SAA. The measurement of battery cell performance was carried out using a CV meter to determine the electrochemical performance and measure the battery capacity.

RESULTS AND DISCUSSION

Activated Carbon Production

Coconut shell (**Figure 1a**) with a carbon content of about 74.3% presents good potential as a carbon material (Bledzki, Mamun, & Volk, 2010). The pyrolysis process decomposes organic compounds such as cellulose and lignin as well as volatile substances by heating in small amounts of oxygen and without the presence of other chemical reagents (Sudding, 2013). After the pyrolysis, the coconut shell used in this study would change color to black (**Figure 1b**) indicating the decomposition of hydrocarbon compounds within the coconut shell.

The carbonized coconut shell was first activated before being used as an active material. Chemical activation was done using KOH, whereas physical activation was done using microwave radiation. The activation process was aimed to enlarge the pores and increase the surface area of the activated carbon (Ferrera-Lorenzo, Fuente, Suárez-Ruiz, & Ruiz, 2014). During activation, KOH will bind tar compounds out through the pores so that the pores that are originally covered by impurities will become more open (Marsh & Reinoso, 2006). The opened pores will thereby increase the surface area of the activated carbon to be larger. KOH also acts as a dehydrating agent able to remove trapped water within the pores, further opening it in the process. The chemical reaction that occurs during the carbon activation process using KOH according to Foo and Hameed (Foo & Hameed, 2012) entails that KOH will be reduced to potassium metal as shown in equation 1.

$$6\ KOH + C \rightarrow 2\ K + 3\ H_2 + 2\ K_2CO_3 \qquad (1)$$

Physical activation with microwave radiation takes place through the mechanism of dipolar polarization and ionic conduction. Physical activation with microwaves was aimed to increase the surface area and enlarge the pores.

Figure 1. (**a**) Coconut shell before carbonization and (**b**) Coconut shell after carbonization

Active Anode Material Synthesis

The anode active material is an important component in the battery. The anode is the negative electrode where the half-cell oxidation reaction occurs, releasing electrons to the external circuit. Coconut shell activated carbon that had been made was used as an active material by adding LiOH.

The active material was synthesized using other materials such as PEG 6000. Polyethylene glycol (PEG) 6000 is a polymer that functions as a size controller that produces particles with a high surface area and prevents the agglomeration of particles (Fey, Huang, Kao, & Li, 2011). The addition of other materials during the synthesis of the active material such as citric acid serves to overcome the LiOH agglomeration that could have potentially occur in Li/AC 3/1 and Li/AC 4/1 materials. Citric acid served as a pH controller as well. The heating at a temperature of 100°C would promote the production of a thick solution or gel. The gel formation process that occurred is a condensation reaction in which 2 or more compounds combine to form larger molecules.

The resulting gel was calcined for 3 hours at a temperature of 300°C. The calcination was aimed to remove organic molecules that were still present in the synthesized product (Danks, Hall, & Schnepp, 2016). The product acquired from the calcination was a black powder that comes from the color of activated carbon.

Electrical Conductivity Test

The synthesized active material was characterized for its inductance, capacitance, and resistance (LCR) to determine the electrical conductivity of the material. The electrical conductivity values of the materials were calculated from the antilog of the intercept in the plateau area equation (**Figure 2**) and are shown in **Table 1**. The plateau area is an area with a y value (conductivity log) that has a very small or stable increase with respect to changes in x (frequency log).

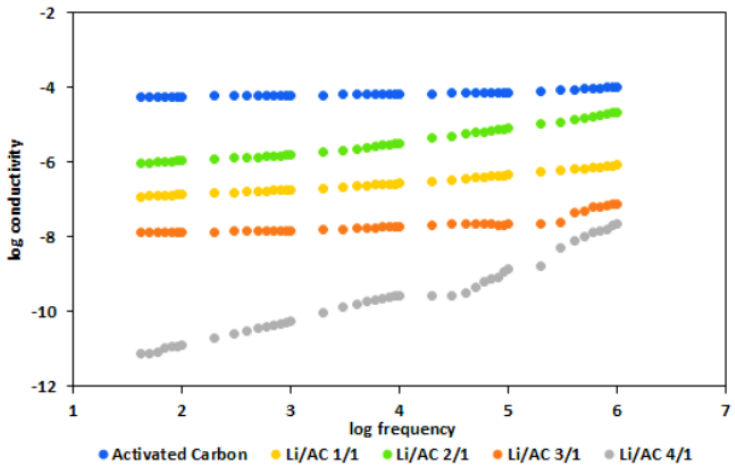

Figure 2. Frequency-dependent electrical conductivity graph from LCR meter measurement

Table 1. Sample electrical conductivity values from LCR measurements

Sample	Electrical Conductivity (Sm^{-1})
Li/AC 1/1	$7.209x10^{-4}$
Li/AC 2/1	$2.064x10^{-3}$
Li/AC 3/1	$1.770 x10^{-4}$
Li/AC 4/1	$1.086x10^{-6}$
Activated Carbon	$5.434x10^{-3}$

Table 1 shows that the material with the highest electrical conductivity was Li/AC 2/1. The electrical conductivity increased from LiOH ratio composition of 1 to 2, then decreased with increasing LiOH ratio composition at 3 and 4. This shows that the LiOH composition affects the electrical conductivity of the material.

At Li/AC 1/1 and Li/AC 2/1 products, there is an increase in electrical conductivity due to the even distribution of lithium hydroxide on the surface of the activated carbon pores so that electrons flow in the anode material (Pratiwi, Sugiarti, & Wijaya, 2017). Thus, the electrical conductivity value increases. Meanwhile, the electrical conductivity which decreased with the addition of LiOH composition in the ratios of 3 and 4 is thought to have occurred due to the colloidal agglomeration of LiOH. This can be seen from the calcination products of Li/AC 3/1 and Li/AC 4/1 which had formed lumps. Agglomeration causes the particle size to become larger and the pores become tight so that lithium hydroxide cannot be accommodated on the surface of the activated carbon pores. The large particle size causes the resistance to increase, consequently, the electrical conductivity decreases because the resistance is inversely proportional to the electrical conductivity (Subhan, 2011).

The electrical conductivity of Li/AC 2/1 was compared to the activated carbon without LiOH addition. The results as shown in **Table 1** suggest that the electrical conductivity of the activated carbon was slightly higher than that of the Li/AC 2/1 active material. It is presumed to be attributed to the formation of larger pores in the activated carbon allowing for electron mobility not to be hampered. Whereas, in Li/AC 2/1 material smaller pore size was observed as demonstrated by the SAA analysis presented in **Table 3**.

Active Material Characterization

Based on the results of the electrical conductivity test, the materials with the highest conductivity value, namely Li/AC 2/1 and activated carbon, were applied as anode active materials arranged into battery cells. These materials were characterized using FTIR spectroscopy, SAA, XRD, and CV meter.

FTIR Characterization

The IR spectrum of the Li/AC 2/1 material was compared to the spectrum of activated carbon to determine whether the material was successfully synthesized as shown in **Figure 3**.

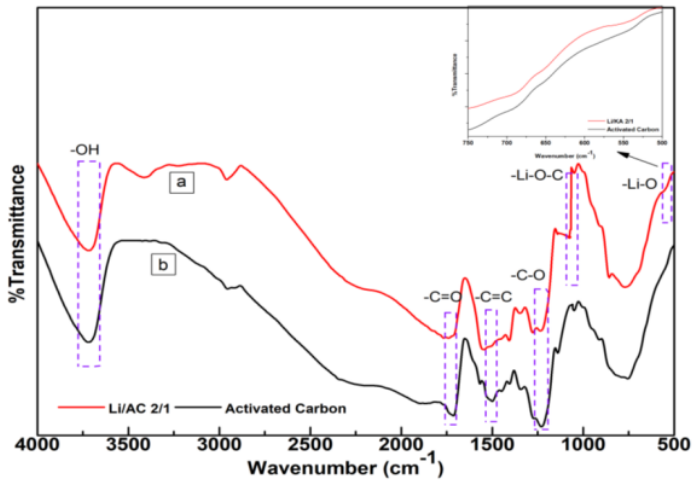

Figure 3. FTIR spectra of activated carbon and Li/AC 2/1

Table 2. Sample functional groups

Functional Group	Sample	
	Activated Carbon	Li/AC 2/1
-C=O	1701	1713
-O-H	3694	3711
-C=C	1491	1500
-C-O	1223	1244
-Li-O-C	-	1075
-Li-O	-	547.5

The spectra of activated carbon showed absorption at a wavenumber of 3694 cm^{-1} indicating a stretching of the –OH functional group derived from cellulose (Liang et al., 2020). The absorption peak at 1491 cm^{-1} indicates the stretching of the aromatic C=C functional group. The stretching vibrations of C=O carbonyl groups such as esters and carboxylic acids appeared in the area around 1701 cm^{-1} (Köseoğlu & Akmil-Ba[25], 2015). The absorption at a wavenumber of 1223 cm^{-1} signifies the stretching of the C-O functional group. The difference in the spectra of activated carbon with Li/AC can be found in the absorption of the Li-O-C group at the wavenumber of 1075 cm^{-1} and the wide absorption in the area of 547.5 cm^{-1} that represents the Li-O vibration (Abdelghanya, ElBatalb, & Ramadanc, 2016). The presence of Li-O-C and Li-O vibrations indicate that the material contains lithium. The electrical conductivity of Li/AC 2/1 is higher than that [40]of activated carbon due to the presence of lithium in the Li/AC 2/1 composite as presented in the FTIR spectrum of Li/AC. **Table 2** shows explicated spectral interpretation of the functional groups contained in the activated carbon and Li/AC 2/1 samples.

[32]***Surface Area Analysis***

Surface area, pore radius, and total pore volume are important properties of a material. Therefore, characterization using a surface area analyzer (SAA) involving the BET method was conducted. The adsorption and desorption [1]otherm curves of activated carbon and Li/AC 2/1 can be seen in **Figure 4**.

Based on the adsorption isotherm curves shown in **Figure 4**, both demonstrated type IV isotherm in which according to Mays (2007), with the formation of multilayer of adsorption and desorption curves, the isotherm produce is quintessential of mesoporous materials.

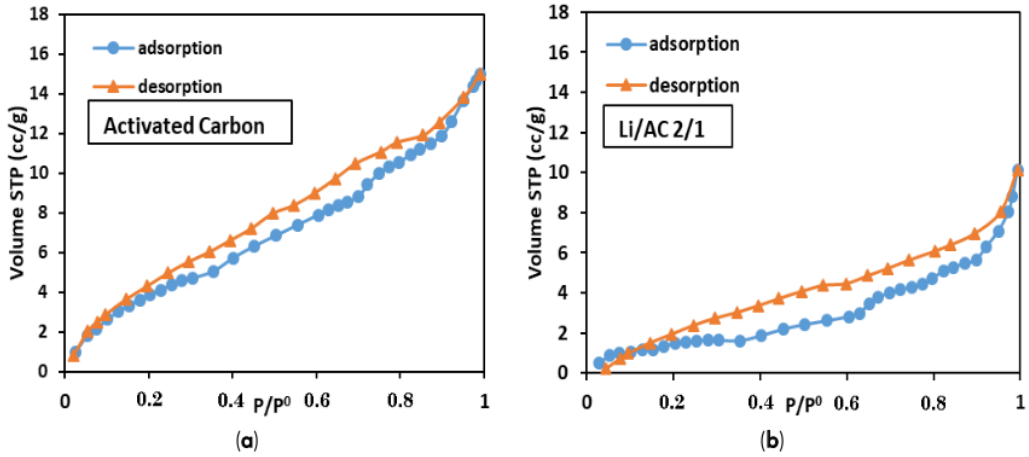

Figure 4. Adsorption desorption isotherm curves of **a**) activated carbon and **b**) Li/AC 2/1

Table 3. [35]Surface area, pore radius, and total pore volume of samples

Sample	[30]Surface Area (m^2g^{-1})	Pore Radius (Å)	Total Pore Volume ($cc.g^{-1}$)
Activated Carbon	17.057	27.816	2.319×10^{-2}
Li/AC 2/1	5.615	10.80	1.566×10^{-2}

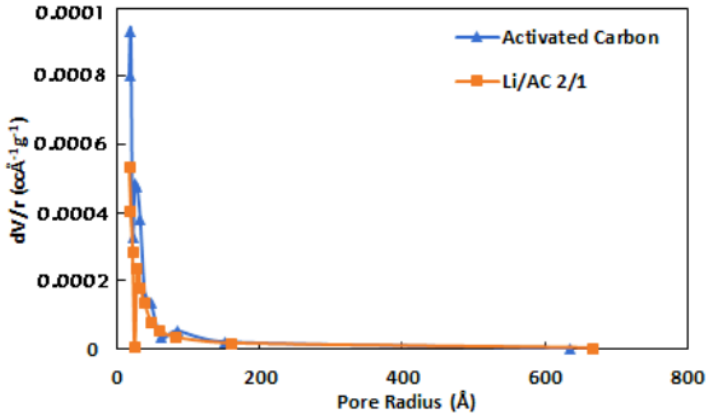

Figure 5. Pore distributions of activated carbon and Li/AC 2/1

Pore size is usually determined by the pore radius (Nimmo, 2004). **Table 3** shows that the pore radius of Li/AC 2/1 material is lower than that of activated carbon. This shows that the pore size for Li/AC 2/1 material is smaller than that of activated carbon. Lower radii suggest more irregular electron conduction paths consequential of an increase in resistance (Li & Lu, 2011). The greater the resistance, the lower the electrical conductivity. Li/AC 2/1 product with a small pore size has a more irregular electron conduction path which increases the electrical resistance. It is because the electric field interaction between one pore and another for Li/AC 2/1 product is strong so that the path for electrons flows hard. As a result, the electrical conductivity decreases (Ke, Cheng-Feng, & Zhen-Gang, 2007). This is in accordance with the results of the electrical conductivity test shown in **Table 1** where the electrical conductivity of Li/AC 2/1 was less than that of activated carbon.

Li/AC 2/1 material had a pore volume of 5.35 x 10^{-4} ccg^{-1} and a pore radius of 16.83 Å. Meanwhile, activated carbon had the highest pore volume at 8 x 10^{-4} ccg^{-1} with a pore radius of 16.85 Å as shown in **Figure 5**. A higher pore size with a higher number or volume of pores is conjectural of fewer inter-porous cavities than materials with a lower pore radius and lower pore volume. The number of voids between pores can be related to the porosity value where porosity is the ratio between the volume of voids per total volume. High porosity causes the measured resistance to be greater implying that fewer electrons can flow (Tristiana, Sembiring, & Simanjuntak, 2017).

The results of the SAA analysis presented in **Table 3** indicate that the surface area of Li/AC 2/1 was smaller than that of activated carbon. Surface area affects the capacity that a material can have. Materials with a high surface area will have a high capacity because a large surface area can accommodate more ions than a small surface area (K. Yu, Li, Qi, & Liang, 2018). This basis can be proven by measuring the capacity of the battery cells as discussed in **Figure 8**.

XRD Characterization

Observation of the crystal structure and phase identification of activated carbon and Li/AC 2/1 were carried out by XRD and the results are shown in **Figure 6**. The diffraction pattern of the Li/AC 2/1 material was almost similar to that of activated carbon. There was a widening of the diffraction peak at an angle of 2θ = 20° to 30°. Furthermore, there was also a slight shift in the angle of 2θ = 43.98° to 2θ = 43.96° which is the characteristic diffraction peak for activated carbon. There were new diffraction peaks found at angles of 2θ = 32.5°, 34.4°, 37.3°, 41.5°, and 48°. The diffraction pattern was analyzed using X'Pert High Score Plus software. The results showed that the diffraction peaks 2θ = 32.5° and 41.5° matched the JCPDS file number 96-900-8959 indicating the LiOH phase with a tetragonal crystal system. The diffraction peaks at 2θ = 34.4°, 37.3°, and 48° correspond to JCPDS data file number 96-151-6389, namely lithium propanoate with $LiC_3H_5O_2$ composition and monoclinic crystal structure. The detection of lithium propanoate phase which was higher than LiOH is reckoned as a form of impurity. With such case, the electrical conductivity was affected in that it had become smaller than that of activated carbon.

The XRD diffractograms show that the crystallinities of the two samples were still low as the diffraction peaks that appeared were wide or not sharp. The pattern of atomic arrangement in samples with low crystallinity is irregular and affects the electrical conductivity of the material. Electrical conductivity arises because electron easily moves through the crystal lattice (Vijayakumar et al., 2011). If the atomic arrangement is irregular then the movement of electron becomes more difficult so that the electrical conductivity will decrease.

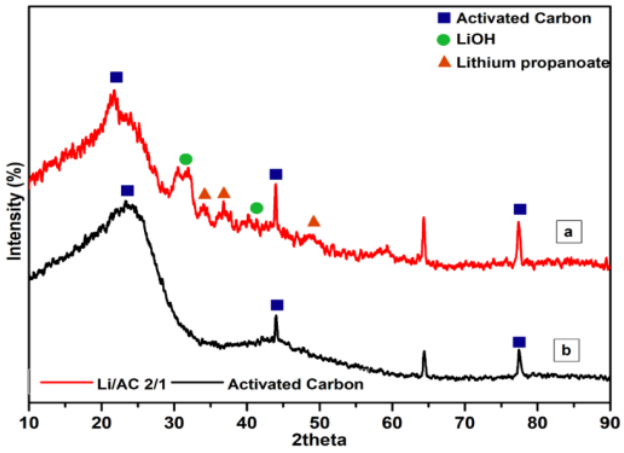

Figure 6. Diffractograms of (**a**) Li/AC 2/1 and (**b**) activated carbon

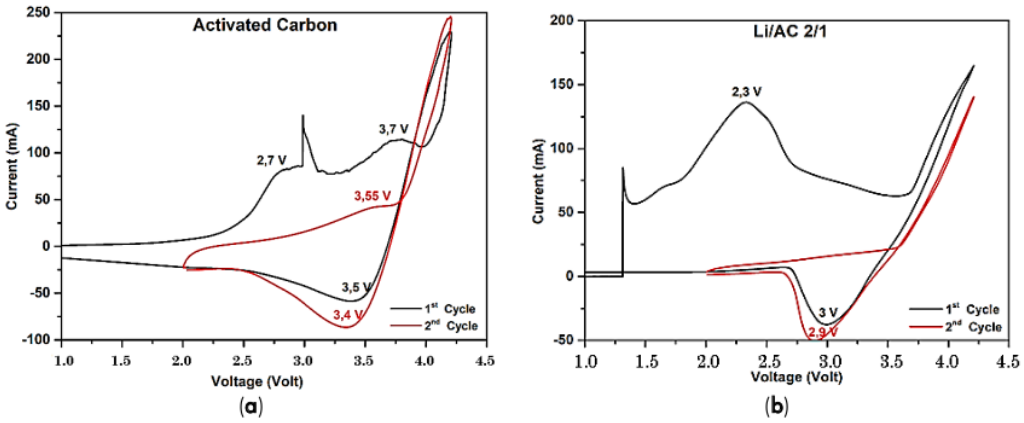

Figure 7. Cyclic voltammetry graphs of (**a**) activated carbon and (**b**) Li/AC 2/1 active materials

Battery Cell Performance

Li/AC 2/1 and activated carbon which had the highest electrical conductivities were arranged into battery cells. The performances of the battery cells were analyzed using cyclic voltammetry and measurement of battery capacity. Cyclic voltammetry test was aimed to determine the electrochemical performance of battery cells during the charging and discharging process.

Figure 7 shows the relationship between the input voltage and the current measured as the output. In the first cycle, there were 2 peaks in both samples which were anodic peak and cathodic peak. The presence of a pair of redox peaks in the first cycle indicates that the battery cell reaction was reversible. In the activated carbon sample, anodic peaks appeared at 2.75 V and 3.7 V and cathodic peaks were at 3.55 V. The appearance of anodic peaks indicate the occurrence of electrolyte decomposition, the formation of an SEI layer on the anode surface, and the reaction between lithium ions and functional groups on the activated carbon surface (K. Yu et al., 2018). In the Li/AC 2/1 sample the anodic peak was at 2.3 V and the cathodic peak was at 3 V.

In the second cycle, there was a decrease in peak intensity in both samples. This is due to the formation of solid electrolyte interphase (SEI) layer on the anode surface from electrolyte decomposition (Han et al., 2014). During this cycle, the activated carbon material had a cathodic peak at a voltage of 3.4 V and an anodic peak at a voltage of 3.55 V. The Li/AC 2/1 material formed a cathodic peak with a widening peak at a voltage of 2.9 but no anodic peak was formed. The absence of anodic peaks in the Li/AC 2/1 material could be due to the formation of the SEI layer and irreversible decomposition which inhibited the intercalation process in the second cycle (Su & Dong, 2019).

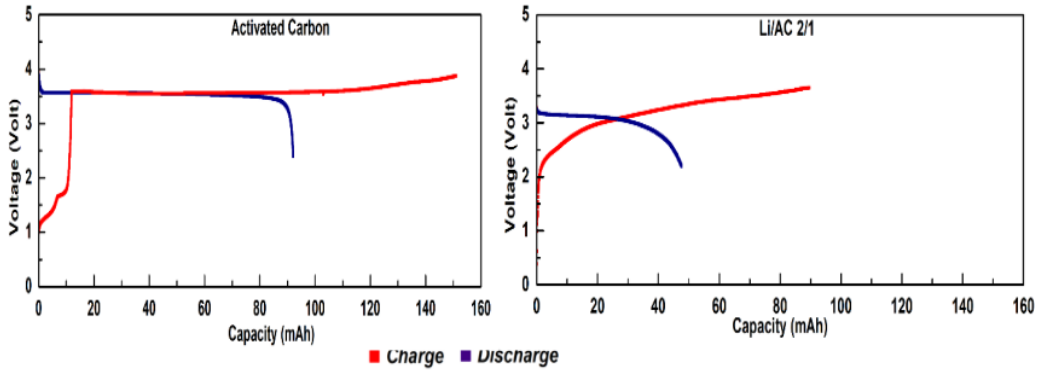

a) b)

Figure 8. Battery cell charge-discharge curves of **a**) activated carbon and **b**) Li/AC 2/1 active materials

The second measurement of battery cell performance was done to measure the capacity of activated carbon and Li/AC 2/1 battery cells to determine their ability to store energy. Measurements were made by a constant current for a certain period of time and the magnitude of the resulting voltage was recorded over time. The value of the voltage and current multiplied by the time will obtain a charge-discharge graph.

The test results shown in **Figure 8** demonstrate a higher capacity for activated carbon than Li/AC 2/1. This shows that the Li^+ ion storage capacity of activated carbon is better than Li/AC 2/1 (Aditya, 2016). These results are in agreement with CV measurements that the current intensity for activated carbon was higher. Based on the results of the LCR test, the electrical conductivity of activated carbon was slightly higher than Li/KA 2/1 with values of 5.434×10^{-3} Sm^{-1} and 2.064×10^{-3} Sm^{-1}, respectively. The electrical conductivity is proportional to the number of electrons flowing (current), meaning that the number of electrons that can flow on activated carbon was more than Li/AC 2/1. This is in accordance with the energy storage capacity of lithium ion batteries in which it depends on the number of lithium ions stored in the electrode structure and the amount that can be moved during the charge and discharge process, as the amount of electron current stored and channeled is proportional to the number of lithium ions that are transferred (Aditya, 2016).

CONCLUSIONS

The LiOH to activated carbon ratio (w/w) in the synthesis of lithium ion battery anode active material which had the highest electrical conductivity value was Li/AC 2/1 with a value of 2.064×10^{-3} Sm^{-1}. The Li/AC 2/1 material showed absorption of the Li-O-C group at the wavenumber of 1075 cm^{-1} and absorption in the area of 547.5 cm^{-1} indicating Li-O vibration. Surface area analysis (SAA) presented that Li/AC 2/1 had a surface area of 5.615 m^2g^{-1}. The crystallinity of the Li/AC 2/1 active material was low shown by the widening of the diffraction peaks at 2θ 10° to 35° due to the presence of activated carbon. The charge and discharge capacities for Li/AC 2/1 were 91.103 mAh and 47.580 mAh.

ACKNOWLEDGMENTS

The authors would like to thank Universitas Diponegoro for the financial support with grant number 118-12/UN7.6.1/PP/2021 (World Class Research Universitas Diponegoro Kategori B scheme) in the fiscal year 2021.

REFERENCES

Abdelghanya, , ElBatalb, H., & Ramadanc, R. (2016). Structural role of Li_2O or LiFon spectral properties of cobalt doped borate glasses. *Journal of King Saud University - Science*, *29*(4), 510-516.

Aditya, N. S. T. (2016). Analysis of hydrothermal temperature effect on anode MnO_2 synthesis process against morphology and electrochemical of lithium ion battery. (*Undergraduate Thesis*), Sepuluh Nopember Institute of Technology Surabaya.

Bledzki, A. K., Mamun, A. A., & Volk, J. (2010). Barley husk and coconut shell reinforced polypropylene composites: The effect of fibre physical, chemical, and surface properties. *Composites Science and Technology*, *70*(5), 840-846.

Corti, H., Crovetto, R., & Fernández-Prini, R. (1979). Aqueous solutions of lithium hydroxide at various temperatures: Conductivity and activity coefficients. *Journal of Solution Chemistry*, *8*(12), 8 -908.

Danks, A. E., Hall, S. R., & Schnepp, Z. (2016). The evolution of 'sol–gel' chemistry as a technique for materials synthesis. *Materials Horizons*, *3*(2), 91-112.

Ferrera-Lorenzo, N., Fuente, E., Suárez-Ruiz, I., & Ruiz, B. (2014). KOH activated carbon from conventional and microwave heating system of

a macroalgae waste from the Agar–Agar industry. *Fuel processing technology, 121*,25-31.

Fey, G. T.-K., Huang, K.-P., Kao, H.-M., & Li, W.-H. (2011). A polyethylene glycol-assisted carbothermal reduction method to synthesize $LiFePO_4$ using industrial raw materials. *Journal of Power Sources, 196*(5), 2810-2818.

Foo, K., & Hameed, B. (2012). Coconut husk derived activated carbon via microwave induced activation: Effects of activation agents, preparation parameters and adsorption performance. *Chemical Engineering Journal, 184*, 57-65.

Han, S.-W., Jung, D.-W., Jeong, J.-H., & Oh, E.-S. (2014). Effect of pyrolysis temperature on carbon obtained from green tea biomass for superior lithium ion battery anodes. *Chemical Engineering Journal, 254*, 597-604.

Ke, Z., Cheng-Feng, L., & Zhen-Gang, Z. (2007). Measurement of electrical conductivity of porous titanium and Ti6Al4V prepared by the powder metallurgy method. *Chinese Physics Letters, 24*(1), 187.

Kim, T., Jo, C., Lim, W.-G., Lee, J., Lee, J., & Lee, K.-H. (2016). Facile conversion of activated carbon to battery anode material using microwave graphitization. *Carbon, 104*, 106-111.

Köseoğlu, E., & Akmil-Başar, C. (2015). Preparation, structural evaluation and adsorptive properties of activated carbon from agricultural waste biomass. *Advanced Powder Technology, 26*(3), 811-818.

Li, B., & Lu, X. (2011). The effect of pore structure on the electrical conductivity of Ti. *Transport in Porous Media, 87*(1), 179-189.

Liang, Q., Liu, Y., Chen, M., Ma, L., Yang, B., Li, L., & Liu, Q. (2020). Optimized preparation of activated carbon from coconut shell and municipal sludge. *Materials Chemistry and Physics, 241*, 122327.

Mays, T. (2007). A new classification of pore sizes. *Studies in surface science and catalysis, 160*(Characterization of Porous Solids VII), 57-62.

Nimmo, J. R. (2004). Porosity and pore size distribution. *Encyclopedia of Soils in the Environment, 3*(1), 295-303.

Pratiwi, D. E., Sugiarti, S., & Wijaya, M. (2017). The effect of adding lithium hydroxide (LiOH) on the conductivity of chitosan membranes for its application in lithium polymer batteries. *Paper presented at the Seminar Nasional LP2M UNM*.

Su, R., & Dong, X. (2019). Preparation and electrochemical properties of bamboo-based carbon for lithium-ion-battery anode material. *International Journal of Electerochemical Science, 14*(3), 2452-2461.

Subhan, A. (2011). *Fabrication and characterization of $Li_4Ti_5O_{12}$ for materials ceramic lithium battery anode.* (*Thesis*), Indonesia University, Jakarta.

Sudding, M. (2013). Production and quality analysis of coconut shell charcoal briquettes in terms of starch content. *Jurnal Chemica, 14*(1), 74-83.

Susana, H., & Astuti, A. (2016). Effect of LiOH concentration on electrical properties of lithium battery anodes based on candlenut shell activated carbon. *Jurnal Fisika Unand, 5*(2), 136-141.

Tristiana, A. L., Sembiring, S., & Simanjuntak, W. (2017). Microstructure and Electrical Conductivity of Cordierite Ceramic with Addition of Magnesium Oxide (0, 10, 15 wt%) Based on Silica Rice Husk. *Jurnal Teori dan Aplikasi Fisika, 5*(1), 1-7.

Vijayakumar, M., Kerisit, S., Rosso, K. M., Burton, S. D., Sears, J. A., Yang, Z., Graff, G. L., Liu, L., Hu, J. (2011). Lithium diffusion in $Li_4Ti_5O_{12}$ at high temperatures. *Journal of Power Sources, 196*(4), 2211-2220.

Yu, K., Li, J., Qi, H., & Liang, C. (2018). High-capacity activated carbon anode material for lithium-ion batteries prepared from rice husk by a facile method. *Diamond and Related Materials, 89*, 139-145. doi: 10.1016/j.diamond.2018.04.019

Yu, X., Zhang, K., Tian, N., Qin, A., Liao, L., Du, R., & Wei, C. (2015). Biomass carbon derived from sisal fiber as anode material for lithium-ion batteries. *Materials Letters, 142*, 193-196.

Yuningsih, L. M., & Mulyadi, D. (2016). The effect of activation of active carbon from corn cob and shell on conductivity value. *Santika (Scientific Journal of Science and Technology), 6*(2), 531-536.

LiOH/Coconut Shell Activated Carbon Ratio Effect on the Electrical Conductivity of Lithium Ion Battery Anode Active Material

ORIGINALITY REPORT

17%	14%	12%	7%
SIMILARITY INDEX	INTERNET SOURCES	PUBLICATIONS	STUDENT PAPERS

PRIMARY SOURCES

1	iwaponline.com Internet Source	1%
2	digiresearch.vut.ac.za Internet Source	1%
3	Yulia Arinicheva, Michael Wolff, Sandra Lobe, Christian Dellen et al. "Ceramics for electrochemical storage", Elsevier BV, 2020 Publication	1%
4	media.neliti.com Internet Source	1%
5	Krishna Kumar Jaiswal, Chandrama Roy Chowdhury, Deepti Yadav, Ravikant Verma et al. "Renewable and sustainable clean energy development and impact on social, economic, and environmental health", Energy Nexus, 2022 Publication	1%
6	bioresources.cnr.ncsu.edu Internet Source	1%

7	Submitted to Universiti Teknologi MARA Student Paper	1 %
8	Submitted to Imperial College of Science, Technology and Medicine Student Paper	1 %
9	jurnal.fmipa.unila.ac.id Internet Source	1 %
10	www.journalmt.com Internet Source	1 %
11	www.omicsonline.org Internet Source	1 %
12	M Jumnahdi, W B Kurniawan, R G Mahardika, Ipi, M E Saputra. "Fabrication Of Lithium-Carbon Composite Material From Pepper Peel Waste As Battery Electrodes", IOP Conference Series: Earth and Environmental Science, 2021 Publication	1 %
13	Submitted to Universiti Teknologi Petronas Student Paper	1 %
14	espace.curtin.edu.au Internet Source	<1 %
15	dr.ntu.edu.sg Internet Source	<1 %
16	dalspace.library.dal.ca Internet Source	<1 %

17	www.ukm.my Internet Source	<1%
18	Cho, Jeong-Hyun, and S. Tom Picraux. "Silicon Nanowire Degradation and Stabilization during Lithium Cycling by SEI Layer Formation", Nano Letters Publication	<1%
19	cyberleninka.org Internet Source	<1%
20	pt.scribd.com Internet Source	<1%
21	asr.urmia.ac.ir Internet Source	<1%
22	electrochemsci.org Internet Source	<1%
23	www.frontiersin.org Internet Source	<1%
24	Submitted to Universitas Jenderal Soedirman Student Paper	<1%
25	"Green Adsorbents to Remove Metals, Dyes and Boron from Polluted Water", Springer Science and Business Media LLC, 2021 Publication	<1%
26	onlinelibrary.wiley.com Internet Source	<1%

27	Submitted to Istanbul Aydin University Student Paper	<1 %
28	journal.uinjkt.ac.id Internet Source	<1 %
29	Refka Andoulsi-Fezei, Nasr Sdiri, Karima Horchani-Naifer, Mokhtar Férid. "Dielectric properties of calcium-substituted lanthanum ferrite", Journal of Asian Ceramic Societies, 2020 Publication	<1 %
30	Houskova, V.. "Efficient gas phase photodecomposition of acetone by Ru-doped Titania", Applied Catalysis B, Environmental, 20090715 Publication	<1 %
31	etd.lsu.edu Internet Source	<1 %
32	prr.hec.gov.pk Internet Source	<1 %
33	www.researchgate.net Internet Source	<1 %
34	Budiyono Budiyono, Aldi Budi Riyanta, Siswo Sumardiono, Bakti Jos, Iqbal Syaichurrozi. "Optimization of Parameters for Biogas Production from Bagasse Using Taguchi	<1 %

	Method", Polish Journal of Environmental Studies, 2021 Publication	
35	Submitted to Texas A & M University, Kingville Student Paper	<1 %
36	edoc.ub.uni-muenchen.de Internet Source	<1 %
37	Murphy, Samuel T., Philippe Zeller, Alain Chartier, and Laurent Van Brutzel. "Atomistic Simulation of the Structural, Thermodynamic, and Elastic Properties of Li_2TiO_3", The Journal of Physical Chemistry C, 2011. Publication	<1 %
38	Silviana Silviana, Amar Ma'ruf, Febio Dalanta. "Silicone for Lithium-Ion Battery Anode Derived from Geothermal Waste Silica through Magnesiothermic Reduction and Double Stages in Acid Leaching", Defect and Diffusion Forum, 2022 Publication	<1 %
39	article.sciencepublishinggroup.com Internet Source	<1 %
40	atrium.lib.uoguelph.ca Internet Source	<1 %
41	ebin.pub Internet Source	<1 %

42	upcommons.upc.edu Internet Source	<1%
43	www.research-collection.ethz.ch Internet Source	<1%
44	Abdulbari A. Ahmad, Marwan Al-Raggad, Noama Shareef. "Production of activated carbon derived from agricultural by-products via microwave-induced chemical activation: a review", Carbon Letters, 2021 Publication	<1%

Exclude quotes	Off	Exclude matches	Off
Exclude bibliography	Off		